IEEE Access
Multidisciplinary | Rapid Review | Open Access Journal

Received November 30, 2018, accepted December 23, 2018, date of publication January 10, 2019, date of current version February 4, 2019.

Digital Object Identifier 10.1109/ACCESS.2019.2891954

A Spiral Seal Method in the Lunar Regolith for Chang'E-5 Drill: Seal Design and Experiment

WEIWEI ZHANG, HUAZHI CHEN, WEIKANG JIANG, RONGKAI LIU, AND SHENGYUAN JIANG
State Key Laboratory of Robotics and System, Harbin Institute of Technology, Harbin 150001, China

Corresponding author: Shengyuan Jiang (jiangshy@hit.edu.cn)

This work was supported by the National Natural Science Foundation of China under Grant 51575122.

ABSTRACT In the Chang'E-5 mission of the lunar regolith drilling, the gap between the rotary drill bit and the sheath is required to be sealed. In view of the particularity of the lunar subsurface operation, a spiral seal method is proposed based on the analysis of the particles flow state in the clearance, which is made up of the spiral ribs on the inner surface of the drill bit and the friction interface on the outer surface of the sheath. The drilling and sampling simulation is carried out using discrete element method, which verifies the feasibility of the spiral seal in principle. For the test of sealing performance, a test system was developed and drilling and sampling experiments were carried out with several groups of sealing components that have different structure parameters. The test results show that the proposed spiral seal method solves the problem of regolith leakage well in the drilling and sampling process, and it will contribute to the design of the Chang'E-5 drill.

INDEX TERMS Chang'E-5, lunar regolith drilling, spiral seal method, discrete element method, test verification.

I. INTRODUCTION

There are many difficulties in the planetary drilling missions such as unknown regolith properties, low power, limited envelop and so on [1]. For coring soil sample and retaining the stratification information, many laboratories have designed artful drilling device.

Soviet has successful obtained lunar regolith sample by Luna 16, Luna 20 and Luna 24 from 1970 to 1976. The series of Luna all use drill to penetrate regolith and use flexible tube to collect soil sample [2]. Luna series have not got expected depth due to the low adaptability [3], [4]. During 1969∼1972, American Apollo programs have sent some astronauts to lunar. By a Hand-held rotary impact electric drilling rig (ALSD) with a hollow drill stem, Apollo 15/16/17 obtains the lunar regolith sample which measured approximate 3m length [5]. The drilling regulation of ALSD can be adjusted to adapt working condition [6], [7]. Italy space agency Mars exploration program suggested a deep automatic drilling sampling system with multi rod in 2003. By assembling numbers of drilling stems, it can approach 2m depth [8]. In 2004, the ESA launched a comet ''Rosetta'' detector [9]–[11], carrying the SD2 sampler for a rotary drilling to collect soil samples from the depth of 200mm below the surface of the comet. MIT has developed a test device for sampling the surface of Mars. It can estimate soil properties based on the mechanical and soil interaction dynamic model [12]. In 2012, the Mars Science Laboratory (MSL), which successfully landed on Mars, carried a set of brachial load shallower drilling sampler to carry out the analysis of soil samples and rock samples on the Martian surface [13], [14]. The sampler can reach the depth of 50mm. Honeybee Robotics has developed CRUX, MARTE and DAME drilling and testing device for lunar and Mars exploration [15]–[17]. DAME can distinguish the blocking rotation, sticking the drilling and hard target by extracting vibration signal of drill rod [18], [19]. Honeybee Robotics has developed the Icebreaker drilling sampling device, using the rotary percussion drilling regulation, the test drill tool and the sample collection transfer device equipped with the temperature measuring function. It has the function of automatically identifying some fault drilling conditions and starting the corresponding recovery program [20].

The particularity of sampling on celestial bodies makes it special for technology. As for sealing, normal sealing material can't adapt to the terrible environment and normal seal methods can't s be used because of the limited condition. For the Chang'E-5 drill, this paper suggests a spiral seal method to seal the rotary parts and the method feasibility is verified by the theoretical analysis, numerical simulation and experiment test.

The remainder of this paper is organized as follows. Section II introduces the working principle and design of the spiral seal. Sealing simulation is presented in Section III. In Section IV, sealing experiments are conducted to evaluate sealing performance. Finally, Section V concludes this paper.

II. SEAL DESIGN AND PRINCIPLE

A. BACKGROUND

Fig. 1 is the lunar regolith drilling and sampling process of Chang'E-5 drill. The drill can penetrate lunar regolith and the flexible tube covering in the rigid tube was used to sampling the regolith [21]. The drilling stem is hollow which contains a rigid tube concentric with the stem. The flexible tube covers rigid tube outside and overturns into the inside of tube. Drill stem penetrates into lunar regolith with rotation while the rigid tube does not rotate. With the increase of penetrating depth, the regolith is cored into flexible tube gradually.

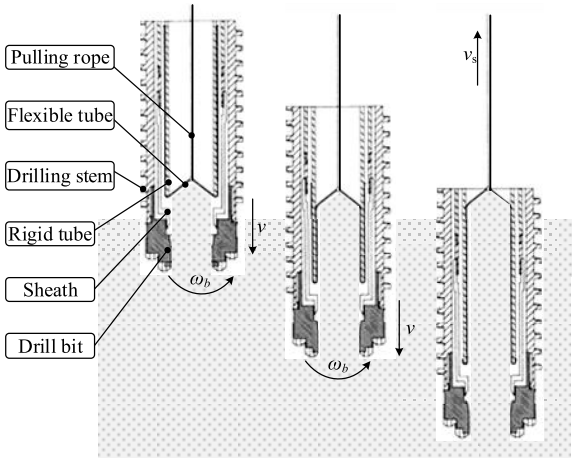

FIGURE 1. Lunar regolith drilling and sampling process.

For protecting the flexible tube, a sheath between stem and rigid tube was designed and lead to a gap between the sheath and the drill bit. For preventing the lunar regolith get into the drill, it's necessary to make a rotary seal for the gap between sheath and drill bit.

B. LUNAR REGOLITH

The granularity of the lunar soil is similar to the silt, and the separation is generally poor. The particle size distribution of lunar soil is very wide. The particle diameter is mainly less than 1mm, the most of the particles are between 30μm and 1mm in diameter. The median particle size is between 40μm-130μm, and the average particle size is about 70μm. The particle morphology of the lunar soil is highly variable and appears from the sphere to the extreme angle as shown in Fig. 2, but the elongated and angular shape particles are more common.

The zigzag particles interlock that make it difficult to glide, and it will lead to a larger internal friction angle of lunar regolith, Tab. 1 is the best estimated value of internal friction angle φ and cohesive force c for lunar soil at different depths [22]. This causes the lunar regolith to be almost similar to the solid rock in resisting the penetration of external objects so that the drilling sampler or the sampling shovel require greater pressure to take a smooth sampling [21]. Besides that, the lunar regolith with larger morphological and size variation make it also difficult to seal.

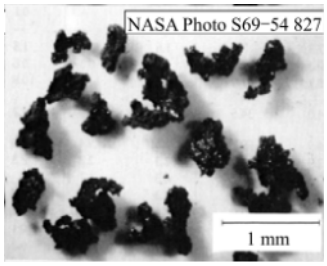

FIGURE 2. Particles shape of the Lunar regolith [24].

TABLE 1. Best estimated value of internal friction angle φ and cohesion force c of lunar soil at different depths.

Depth	Cohesive force c/kPa		Internal friction angle φ/(°)	
/cm	range	average	range	average
0-15	0.44-0.62	0.52	41-43	42
0-30	0.74-1.1	0.90	44-47	46
30-60	2.4-3.8	3.0	52-55	54
0-60	/	1.3-1.9	48-51	/

C. SPIRAL SEAL DESIGN

With a gap when fully use the way to deal with the drill bit and the sheath, and the gap size will have great influence on the sealing performance. If the gap has a small size, it is easy to cause a small amount of fine particles to stagnate and cause the rotational torque to rise. Conversely, if the gap has a large size, a large amount of soil particles will flow into the gap, resulting in an increase in soil leakage.

For the above analysis, the best solution is to increase the gap size while controlling the influx of particles. Thus, a sealing scheme for lunar regolith is envisaged, a narrow slot entrance with a small gap size δ_s was designed to prevent large particles from entering and block most of the particles, and a wide chip groove with a larger gap size δ is arranged above the narrow slot entry to accommodate tiny particles. Based on the above idea, the chip groove was designed as a multi-layer structure to prevent particles from entering effectively. The idea of layered seal is extended, and the chip groove of each layer is made into spiral grooves. On the one hand, the particles can be layered sealed, and on the other hand, particles can be discharged from the chip groove. The process of design thought is shown in the Fig. 3.

Because of terrible environment, such as low vacuum, high temperature, normal seal methods like seal ring are unsuited, a spiral seal method was proposed, as shown in Fig. 4.

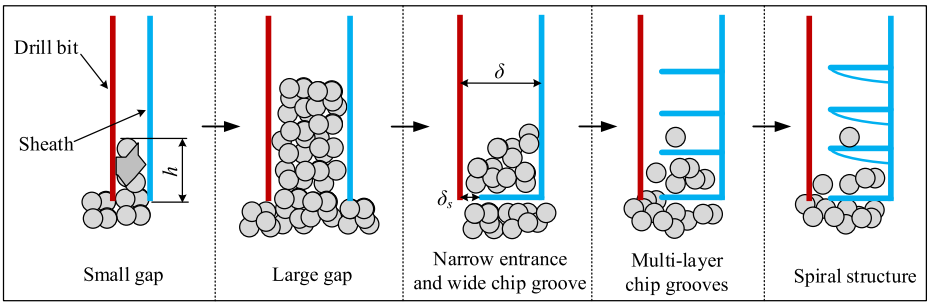

FIGURE 3. Design idea of the spiral seal.

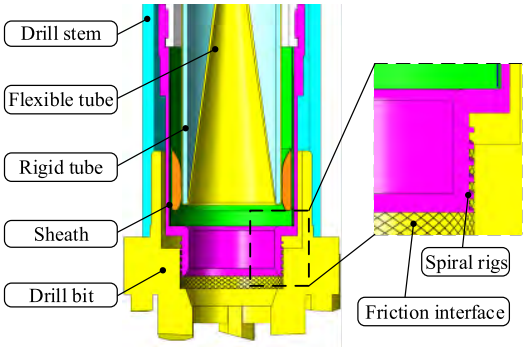

FIGURE 4. Spiral seal structure.

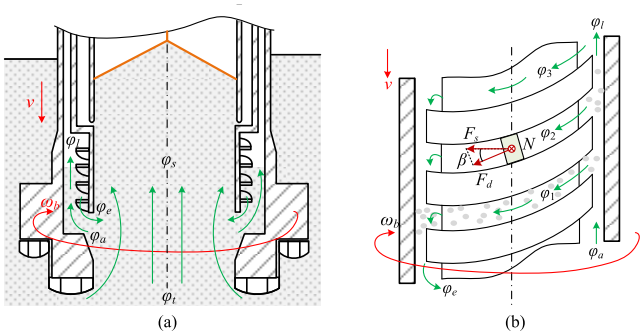

FIGURE 5. Chips flow in the drilling and sampling process. (a) Flow rates in drilling and sampling process. (b) Particles force and flow on spiral rigs.

The spiral seal structure is made up of the spiral ribs on the inner surface of the drill bit and the friction interface on the outer surface of the sheath. There is a relative rotational motion between drill bit and the sheath that makes screw deliver regolith particles downward, so the particle is prevented from getting into the gap between drill bit and sheath.

D. SEALING PRINCIPLE

The chips flow in the drilling process is shown in Fig. 5(a). The total flow rate φ_t of the lunar regolith is divided into φ_s that gets into sheath and φ_a that getting into the clearance. At the same time, same chips are discharged and removed out the spiral groove with a flow rate of φ_e, while the other parts that overflow the spiral seal groove are called leakage with a flow rate of φ_l.

According to the balance of chips flow, the relationships between the chips flow rates can be written as:

$$\varphi_t = \varphi_s + \varphi_a - \varphi_e \tag{1}$$

$$\varphi_l = \varphi_a - \varphi_e \tag{2}$$

As shown in Fig. 5(b), the inner surface of the drill bit is revolving, and the friction force F_s formed by the relative rotation pushes the chip microelement to slide outward in the spiral groove. Due to the restriction of the groove structure, the effective driven force F_d of the microelement must be in the tangent direction of the spiral groove, and it can be calculated as:

$$F_d = F_s \cos\beta = \mu_p N \cos\beta \tag{3}$$

where μ_p is the friction factor between the inner surface of the drill bit and the lunar regolith; N is the normal force acting on the microelement of lunar regolith applied by the drill bit, and the β represents the helix angle of the spiral rigs.

The particles flow analysis in the gap is shown in Fig. 5(b), the flow rate of the total particles in the gap is φ_a, and same particles with a flow rate of φ_1 move into the first layer of the chip groove, and the particles with a flow rate of φ_2 continues to move upwards. As the same process, the particle flow φ_2 gets into the next layer of chip groove, and at last only a small amount of particle flow φ_l enters the top to form the leakage. For a spiral seal with n layer chips groove, the flow rate φ_e can be deduced as:

$$\varphi_e = \sum_{i=1}^{n} \varphi_i = \eta A \omega_b^2 R_b \tan\beta \tag{4}$$

where η donates the discharging efficient; ω_b represents the rotary speed of the drill bit; A and R_b are respectively the cross section area of the spiral seal and the radius of the inner surface of the drill bit.

In the drilling and sampling process, the sealing effect of the spiral seal is determined by its chip removal ability characterized by the flow rate φ_e. It can be seen that the flow rate φ_e are determined by the rotary speed ω_b, structure parameters (including A, R_b and β) and the discharging efficient η, while the discharging efficient $\eta$is directly determined by the driving force. Therefore, for a great seal performance, this paper mainly investigates the influence of these three factors

of gap size δ, helix angle β and friction factor μ_p on the sealing effect.

III. SEALING SIMULATION

The process of continuous accumulation of lunar regolith particles into the gap can be analyzed by using the discrete element method. In this paper, the classic spherical model was used to simulate the lunar regolith.

A. SIMULATION MODEL

In DEM simulation, the movement of a given particle is governed by Newton's second law:

$$\begin{cases} mv' = mg + \sum F \\ I\omega' = \sum T \end{cases} \tag{5}$$

where m and I are the mass and the rotational inertia of particle i, respectively; v' and ω' are the translational and angular velocity vectors of particle i, respectively; g is the gravitational acceleration; F and T are the contact force and torque generated between particles i and j, respectively.

The contact force F is an important parameter. In this study, the No-slip Hertz–Mindlin contact model is used to describe the interactions among the lunar regolith particles, as shown in Fig. 6.

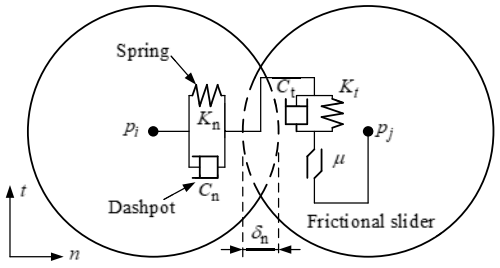

FIGURE 6. Contact force in DEM model.

The forces between the particle and particle are simplified to normal force and tangential force. The normal force is composed of elastic force and damping force. The normal force can be given by

$$F_n = K_n\delta_n + C_n v_n \tag{6}$$

Similarly the tangential force is given by

$$F_t = \min\{\mu F_n, K_t\delta_t + C_t v_t\} \tag{7}$$

The torque among particles can be divided into 3 parts: normal torque T_n, tangential torque T_t and rolling torque T_r.

$$\begin{cases} T_n = RF_n \\ T_t = RF_t \\ T_r = -\mu_d |F_n| R\omega \end{cases} \tag{8}$$

In the contact force model, the subscript n and t indicate normal and tangential direction, respectively. K is the stiffness coefficient of the spring; C is the damping coefficient of the dashpot; δ is the deformation of particle i; v is the velocity of particle i; μ is the coefficient of static friction; R is the radius of particle i. The stiffness and damping coefficient are related to the particle material properties.

TABLE 2. Simulation parameter setting.

	Regolith Particle	Geometry
Poisson's radio	0.5	0.269
Shear modules	3×10^6 Pa	8.23×10^{10} Pa
Density	2500 kg/m^3	7850 kg/m^3
Restitution	0.1	0.1
Static friction	0.8	0.3
Rolling friction	0.08	0.05

According above No-slip Hertz–Mindlin contact model, the EDEM software is used to simulate the particles flow behavior of the lunar regolith in the drilling and sampling process. The input parameters needed in the software contain the Poisson's radio, shear modules, density, restitution, static friction and rolling friction, and these parameters have a clear correspondence with the above parameters in the contact model [25]. The simulation parameters shown in Tab. 2 of lunar regolith particles are determined by matching the mechanical properties of particles mentioned in the reference [23].

Based on the EDEM, the simulation model is set up as Fig. 7. The drilling and sampling conditions are simplified to highlight the particles flow behavior. In order to reduce the particles and simulation computation load, a tube is placed in the center of the drill bit and sheath. The simulation is set to two groups, one with spiral seal (Fig. 7(a)) and the other without spiral seal (Fig. 7(b)), and the comparison can be used to verify the feasibility of the seal scheme.

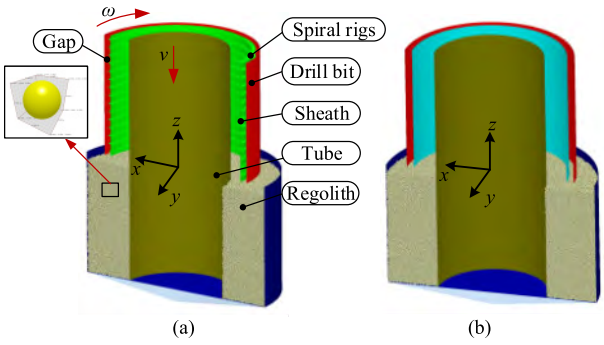

FIGURE 7. Simulation model. (a) Simulation model with spiral seal. (b) Simulation model without Spiral seal.

B. SIMULATION RESULTS

The simulation results is shown in Fig. 8, and the test results show that the lunar regolith particles mass in the gaps of two simulation groups increase with time, while the stacking height of the particles in the simulation group with spiral seal is significantly smaller than the simulation group without spiral seal.

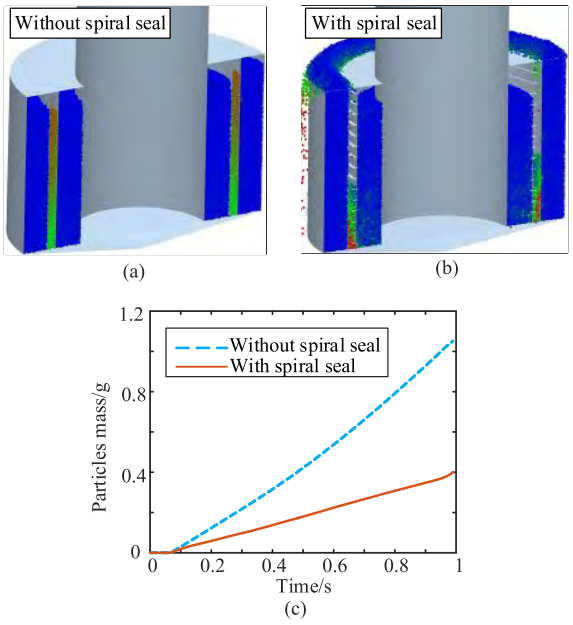

FIGURE 8. The mass of lunar regolith accumulation. (a) Sealing performance without spiral seal. (b) Sealing performance with spiral seal. (c) Comparison particles mass.

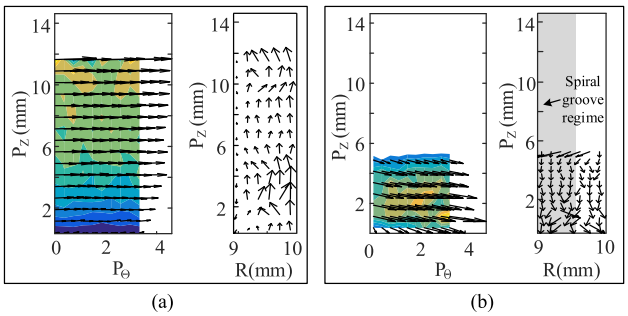

FIGURE 9. Velocity distribution of particles. (a) Particles flow without spiral seal. (b) Particles flow with spiral seal.

The movement of particles in the gap of two experimental groups are shown in Fig. 9. The circular cylindrical clearance is expanded along the circumferential direction to obtain the velocity distribution of the particles in the circumferential direction and the height direction, and the circular cylindrical clearance is projected onto the radius to obtain the distribution of particles in the radius direction and height direction.

In the simulation group without spiral seal, the particles mainly rotate with the drill bit, and its velocities are mainly in the horizontal direction, and the components in the height direction are upward. As a result, particles will quickly accumulate in the gaps. Because of the existence of the spiral rigs, the particles in the gap decelerate obviously and the particles move downward under the guidance of the spiral groove, the downward velocity component is larger than horizontal direction.

The simulation results show the feasibility of spiral seal method, and the particles flow characteristics can be seen from the theoretical analysis is verified.

IV. SEALING EXPERIMENT AND RESULTS

A. EXPERIMENT SETUP

For validating the sealing effect of seal methods with different structure parameters, a test system was setup shown in Fig. 10. The test system consists the rotation module, vibration module and the test module, data acquisition and control system. The rotary module transmits the power of the rotation motor to the drill bit through the tooth belt, which causes the bit to rotate. The vibration module adopts a crank-slider mechanism to make the sheath vibrate in the axial direction. In the test system, the drill bit and sheath can be easily disassembled and replaced for testing different seal methods and structure parameters. In process of the testing, a torque sensor and three load cells are used to record the rotation moment of the drill bit and axis resistance of the sheath, respectively.

In this study, a lunar regolith simulant was used in the drilling test. The raw material of the simulant is Cenozoic alkaline olivine basalt that is dehumidified and crushed into particles of 0.1-1 mm; the particle shape and particle size distribution are shown in Fig. 11. In the process of preparation, the raw material was steeply poured into the container and vibrated to produce a regolith simulant with consistent mechanical properties along the height direction. The bulk density of the regolith simulant is 2.02 g/cm^3 (relative density is 80%).

The sheath is filled with simulant that would be scattered into the gap between sheath and drill bit, and the leakage can be collected and weighed at the end of the test. The rotation moment, axis resistance and the leakage were set as the evaluation index of the sealing performance.

In essence the seal method is a gap coordination of shaft and hole. The styles of shaft and hole affect the rotation movement and the regolith leakage. So it is significant to smooth the movement and minimize the leakage. To optimize the seal design, the experimental groups with different structures parameters of sheath and drill bit are set as shown in Fig. 12. For the sheath, its outer surface was designed in two forms: cylinder screw and smooth. And for the drill bit, its inner surface (Friction interface) was designed in five forms: felt, PTFE, smooth, grid and knurl. The helix angles of spiral rigs are set to 7°, 10° and 14°. The purpose of grid shape is to increase the fraction factor, and it maybe improve the driving effect to increase the number of keyway so that the keyway numbers are set as 12, 18, 37 and 49. As a result, the driving capability of drill bit's inner face may promote. In the experiments, the material of sheath is 45# steel, and the material of drill bit is 40Cr alloy.

Besides the interface of the drill bit and sheath, the size matching of two surfaces is also the goal of experimental investigation, and the parameters of the experimental groups are set as shown in Tab. 3.

The test procedures is carried out in sequence of no-load test, sealing test and performance evaluation:

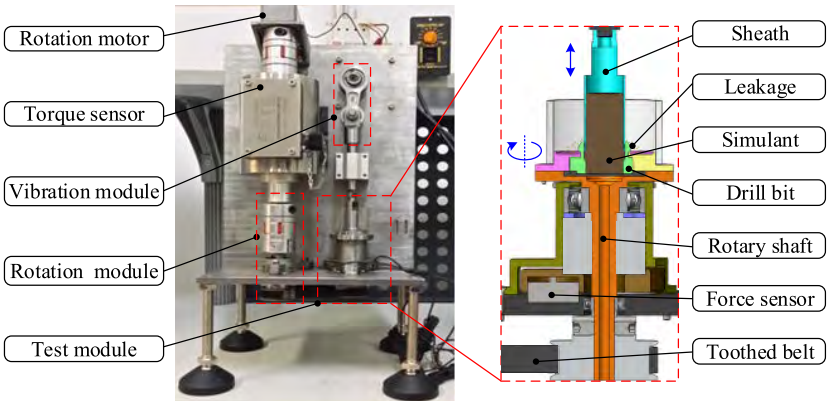

FIGURE 10. Test system.

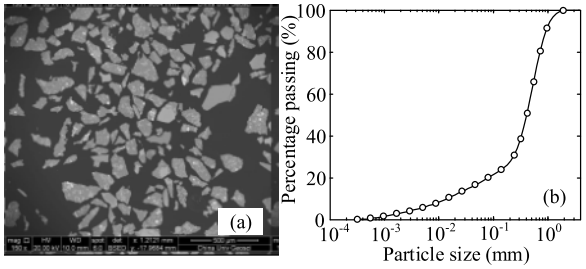

FIGURE 11. Lunar regolith simulant. (a) Particle shape; (b)Particle size distribution.

TABLE 3. Testing group set.

Test groups	Inner surface of drill bit	Outer surface of sheath	Tolerance δs (mm)
G1	Felt	Smooth	0
G2	PTFE	Smooth	0
G3	Smooth	Smooth	0.01
G4	Smooth	Smooth	0.03
G5	Smooth	Smooth	0.05
G6	Smooth	Smooth	0.07
G7	Grid: 12 keyway	Helix angle: 10°	0.05
G8	Grid: 12 keyway	Helix angle: 7°	0.05
G9	Grid: 12 keyway	Helix angle: 14°	0.05
G10	Grid: 18 keyway	Helix angle: 10°	0.05
G11	Grid: 37 keyway	Helix angle: 10°	0.05
G12	Grid: 49 keyway	Helix angle: 10°	0.05
G13	Knurl surface	Helix angle: 10°	0.05

1) No-load test: install the designated drill bit and sheath, the rotary speed of the drill bit is set to 120 rpm, the axial vibration frequency of the sheath is 5 Hz and the vibration amplitude is set to 1.8 mm. After 5 minutes, record the data of rotation moment and resistance;

2) Sealing test: The simulated lunar soil is proportionally allocated and poured into the sheath. Start-up the rotation and vibration motion, and set the motion parameters in accordance with the No-load test. After 2 hours, record the data of rotation moment and resistance;

3) Performance evaluation: after the test, the simulant leakage in the gap was collected and weighted, and the wear of the two surfaces is checked.

TABLE 4. Testing result.

Test groups	Leakage (g)	Peak torque (Nm)	Peak resistance (N)
G1	0.02	2.39	38.17
G2	0.12	0.73	12.59
G3	0.66	2.63	42.22
G4	0.42	2.73	36.07
G5	0.16	0.19	3.41
G6	0.26	2.45	15.98
G7	0.51	0.16	4.42
G8	0.41	0.17	5.80
G9	0.75	0.15	5.42
G10	0.13	0.12	3.89
G11	0	0.09	4.50
G12	0	0.07	4.59
G13	0	0.08	5.05

B. RESULTS AND DISSCUSSION

According to the experimental settings in Tab. 3 and the aforementioned experimental procedures, 13 groups of sealing tests were carried out. In order to ensure the reliability of the data, each group experiments was repeated three times. The test process is shown in Fig. 13 and the test results are shown in Tab. 4. In this section, according to the experimental results, the effects of seal methods, tolerance size, helix angel of the spiral rigs and the type of the friction interface on sealing performance are analyzed in detail.

1) EFFECT OF SEAL METHOD

In order to evaluate the performance of the seal method, G1, G2, G5 and G13 of the test groups were selected, which refers to felt method, PTFE method, smooth method and

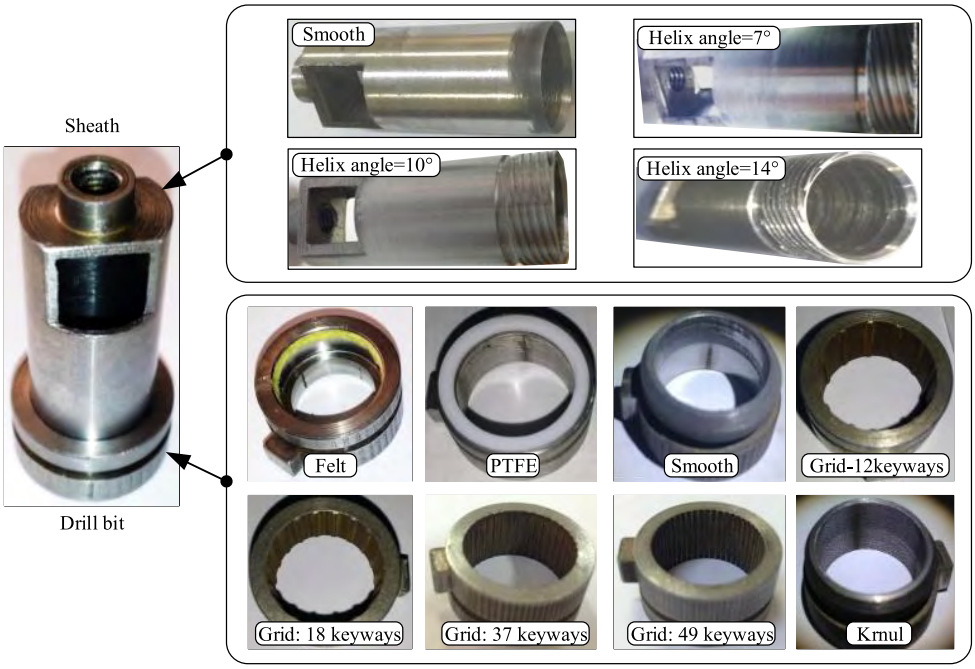

FIGURE 12. Setup of the two interfaces of the drill bit and sheath.

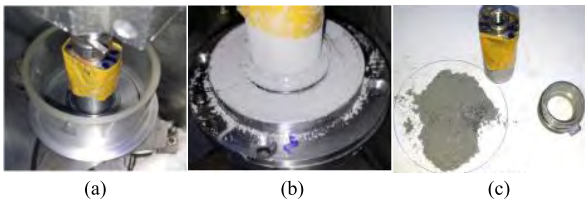

FIGURE 13. Testing process. (a) Initial stage. (b) Finial stage. (c) Leakage.

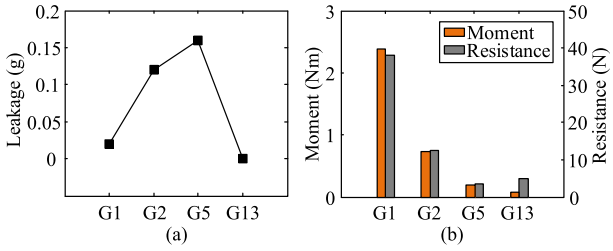

FIGURE 14. Evaluation index vs seal method. (a) Leakage. (b) Moment and resistance.

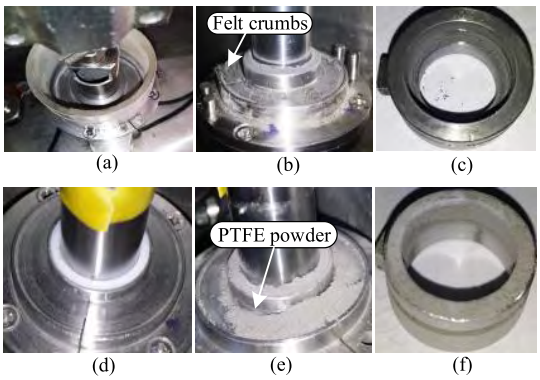

FIGURE 15. Testing result of the felt seal and PTFE seal. (a) Initial stage of felt seal. (b) Final stage of felt seal. (c) Wear state of felt. (d) Initial stage of PTFE seal. (e) Final stage of PTFE seal. (f) Wear state of PTFE.

spiral-knurl method, respectively. The test results of these groups are shown in Fig. 14.

The moment and axial force of felt method reached a large level of 3.89 Nm and 38.17 N, respectively. Besides that, the drill bit stuck several times in the test, so the sealing performance of the felt method was very poor. The PTFE method has a torque of 0.73 Nm, an axial resistance of 12.59 N and a leakage of 0.12 g, and the stuck phenomenon has also occurred in the test, so the sealing effect is also bad.

The test results of the two seal methods are shown in Fig. 15, a lot of simulant have been leaked. In addition, two kinds of sealing materials of felt and PTFE suffered serious wear and tear, and the felt crumbs and PTFE powder were shown in Fig. 15(b) and Fig. 15(e), which eventually led to seal failure. Moreover, these crumbs and powder of sealing materials will contaminate the lunar regolith sample.

Although the rotary moment and axial resistance of smooth method are smaller, the leakage of simulant reaches a larger level of 0.16 g. The spiral-knurl method maintains a relatively low resistance moment and axial resistance, and it can completely seal the simulant (There is no leakage). Therefore, compared with other seal methods, spiral-knurl method has a better performance.

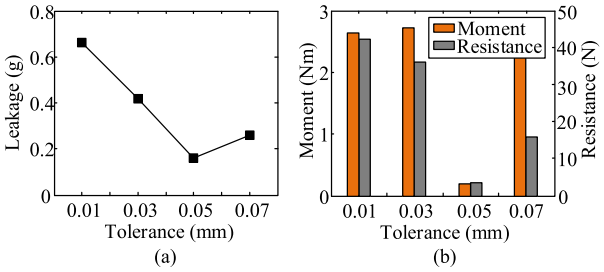

FIGURE 16. Evaluation index vs tolerance. (a) Leakage. (b) Moment and resistance.

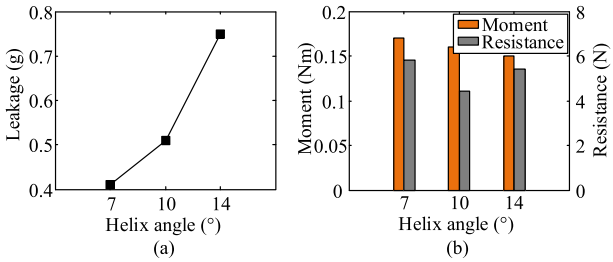

FIGURE 17. Evaluation index vs helix angle. (a) Leakage. (b) Moment and resistance.

2) EFFECT OF TOLERANCE

In order to evaluate the effect of tolerance on sealing performance, G3, G4, G5 and G6 were selected with tolerance of 0.01 mm, 0.03 mm, 0.05 mm and 0.07 mm, respectively. The test results of these groups are shown in Fig. 16.

When the tolerance has a small value, the entrance of simulant particles can easily lead to the drill bit sticking, which leads to large rotation moment and axial resistance. Meanwhile, as a whole, the smaller the gap is, the larger the leakage is. But when the tolerance increases from 0.05 mm to 0.07 mm, the leakage and resistance increase, so the sealing tolerance has a best value to choose.

3) EFFECT OF HELIX ANGLE

In order to evaluate the effect of helix angle on sealing performance, G8, G7 and G9 were selected with helix angle of 7°, 10°, and 14°, respectively. The test results of these groups are shown in Fig. 17.

From the Fig. 17(a), it can be clearly seen that with the increase of helix angle of the spiral rigs, the leakage of the simulant increases gradually. It can be seen from Eq. 3 that the smaller the helix angle, the larger driving force F_d of the lunar regolith particles by the friction surface of the drill bit, and the chip removal efficiency η is improved, thereby effectively reducing the leakage. Therefore, it is more advantageous to choose a smaller helix angle to improve the sealing performance for the spiral seal method.

4) EFFECT OF FRICTION INTERFACE

In order to evaluate the effect of friction interface on sealing performance, G7, G10, G11, G12 and G13 were selected, which refer to grid surface with 12 keyways, grid surface with 18 keyways, grid surface with 37 keyways, grid surface with 49 keyways and the knurl surface, respectively. The test results of these groups are shown in Fig. 18.

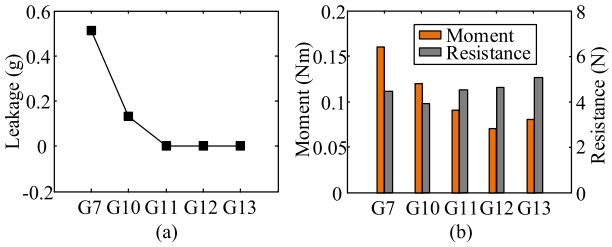

FIGURE 18. Evaluation index vs friction interface. (a) Leakage. (b) Moment and resistance.

It can be seen from Fig. 18(a) that when the keyway number is 12, the leakage of spiral-grid method is even more than that of other seal methods such as smooth method, felt method and PTFE method. Because when the keyway number has small value, there several straight channels with larger space on the inner surface of the drill bit, along which the simulant particles can easily move upward and overflow. Therefore, for the spiral-grid seal method, the keyway number is an important parameter that should be reasonably selected.

As Fig. 18(a) shows, with the increasing keyway number, leakage of the simulant decreases gradually. When the keyway number is larger than 37, there is almost no leakage, and the rotary moment and axial resistance are at a low level as shown in Fig. 18(b). Therefore, the spiral-grid method has a great sealing performance, which is comparable to the spiral-knurl method.

V. CONCLUSION

In the drilling and sampling process of the Chang'E-5 mission, a spiral seal method was proposed to avoid the drill bit and sheath from getting stuck in the lunar regolith. In this method, same spiral rigs are set on the outer surface of the sheath, and the friction interface with larger friction coefficient is designed on the inner surface of the drill bit. The lunar regolith between the drill bit and the sheath is discharged along the spiral groove by the rotary motion of the drill bit to achieve the purpose of sealing. In this paper, the basic principle and feasibility of this kind of spiral seal scheme are preliminarily verified by means of discrete element method. In addition, the experimental study of seal methods was carried out, and the effects of seal methods, tolerance size, and helix angle of the spiral rigs and the friction interface on sealing performance were discussed. Compared with other seal methods, the spiral-knurl method and the spiral-grid method with a larger keyway numbers are feasible choices, which both have low level of sealing resistance and leakage.

In the near future, the spiral seal method will be further validated on the prototype of the Chang'E-5 drill. The research results suggest a feasible scheme for use in the Chang'E-5 and other planetary drilling missions.

REFERENCES

[1] J. W. Keller, N. E. Petro, and R. R. Vondrak, "The lunar reconnaissance orbiter mission—Six years of science and exploration at the moon," *Icarus*, vol. 273, pp. 2–24, Jul. 2016.
[2] J.-L. Bertaux *et al.*, "Discovery of an aurora on Mars," *Nature*, vol. 435, no. 7043, pp. 790–794, Jun. 2005.
[3] T. Ylikorpi, "Preliminary design of an automated lunar soil sampler," Ph.D. dissertation, Dept. Elect. Commun. Eng., Helsinki Univ. Technol., Otaniemi, Finland, 1994.
[4] A. K. Leonovich *et al.*, "Investigation of the physical and mechanical properties of the lunar sample brought by Luna-20 and along the route of motion of Lunokhod 2," in *Proc. 24th Int. Astron. Congr. USSR*, Baku, Azerbaijan, Oct. 1976, pp. 321–322.
[5] R. L. Berry, "Launch window and translunar, lunar orbit, and transearth trajectory planning and control for the Apollo 11 lunar landing mission," in *Proc. 8th Amer. Inst. Aeronaut. Astronaut., Aerosp. Sci. Meeting*, New York, NY, USA, Jan. 1970, pp. 1–17.
[6] J. N. Goswami, D. Lal, M. N. Rao, and T. R. Venkatesan, "Depositional history of Luna 24 drill core soil samples," *Earth Planet. Sci. Lett.*, vol. 44, no. 2, pp. 325–334, Aug. 1979.
[7] S. R. Taylor, *Lunar Science: A Post—Apollo View*. New York, NY, USA: Pergamon, 1975, pp. 8–9.
[8] M. Wu, "Developmentand experimental study of drilling and coring mechanism for lunar soil test system," M.S. thesis, School Mechatron. Eng., Harbin Inst. Technol., Harbin, China, 2014.
[9] A. E. Finzi *et al.*, "SD_2—How to sample a comet," *Space Sci. Rev.*, vol. 128, nos. 1–4, pp. 281–299, Feb. 2007.
[10] K.-H. Glassmeier, H. Boehnhardt, D. Koschny, E. Kührt, and I. Richter, "The Rosetta mission: Flying towards the origin of the solar system," *Space Sci. Rev.*, vol. 128, nos. 1–4, pp. 1–21, Feb. 2007.
[11] N. I. Kömle *et al.*, "Impact penetrometry on a comet nucleus—Interpretation of laboratory data using penetration models," *Planet. Space Sci.*, vol. 49, no. 6, pp. 575–598, May 2001.
[12] W. Hong, "Modeling, estimation, and control of robot-soil interactions," Ph.D. dissertation, Dept. Mech. Eng., Massachusetts Inst. Technol., Cambridge, MA, USA, 2001.
[13] A. B. Okon, "Mars science laboratory drill," in *Proc. 40th Aerosp. Mech. Symp.*, Orlando, FL, USA: NASA Kennedy Space Center, 2010, pp. 1–16.
[14] J. P. Grotzinger *et al.*, "Mars science laboratory mission and science investigation," *Space Sci. Rev.*, vol. 170, nos. 1–4, pp. 5–56, Sep. 2012.
[15] K. Zacny *et al.*, "Honeybee robotics planetary drill systems," in *Proc. Lunar Planet. Sci. Conf.*, League City, TX, USA, 2008, p. 1355.
[16] K. Zacny, "Drilling systems for extraterrestrial subsurface exploration," *Astrobiology*, vol. 8, no. 3, pp. 665–706, Jun. 2008.
[17] G. Paulsen *et al.*, "Robotic drill systems for planetary exploration," in *Proc. AIAA Space Conf. Expo.*, San Jose, CA, USA, 2006, p. 7512.
[18] B. Glass, H. Cannon, M. Branson, S. Hanagud, and G. Paulsen, "DAME: Planetary-prototype drilling automation," *Astrobiology*, vol. 8, no. 3, pp. 653–664, Jun. 2008.
[19] S. M. Statham, "Autonomous structural health monitoring technique for interplanetary drilling applications using laser Doppler velocimeters," Ph.D. dissertation, School Aerosp. Eng., Georgia Inst. Technol., Atlanta, GA, USA, 2011.
[20] B. J. Glass *et al.*, "Robotics and automation for 'icebreaker,'" *J. Field Robot*, vol. 31, no. 1, pp. 192–205, Jan./Feb. 2014.
[21] Y.-C. Zheng, Z.-Y. Ouyang, S.-J. Wang, and Y.-L. Zou, "Physical and mechanical properties of lunar regolith," *Kuangwu Yanshi*, vol. 24, no. 4, pp. 14–19, Dec. 2004.
[22] R. V. Morris, R. Score, C. Dardano, and G. Heiken, *Handbook of Lunar Soils*. Houston, TX, USA: NASA Johnson Space Center, JSC Publ., 1983, p. 914.
[23] D. Zhao *et al.*, "Soil chip convey of lunar subsurface auger drill," *Adv. Space Res.*, vol. 57, no. 10, pp. 2196–2203, May 2016.
[24] J. G. Robert, C. W. Brant, and A. G. Marty, "Development of a high fidelity lunar soil stimulant," *Space Technol. Appl. Int. Forum*, vol. 969, no. 1, pp. 213–220, 2008.
[25] R. D. Mindlin, "Elastic spheres in contact under varying oblique force," *J. Appl. Mech.*, vol. 20, pp. 327–344, Jan. 1953.

WEIWEI ZHANG received the B.S. degrees in mechanical engineering from Beihua University, Jilin, China, in 2012, and the M.S. degree in mechanical engineering from the Harbin Institute of Technology, Harbin, China, in 2014, where he is currently pursuing the Ph.D. degree with the School of Mechatronics Engineering. His research interests include planetary drilling and sampling, and planetary exploration robot systems.

HUAZHI CHEN received the B.S. degrees and the M.S. degree in mechanical engineering from the Harbin Institute of Technology, China, in 2012 and 2014, respectively, where he is currently pursuing the Ph.D. degree with the School of Mechatronics Engineering. His research interests include planetary drilling and sampling, and planetary exploration robot systems.

WEIKANG JIANG received the B.S. degrees in mechanical engineering from the Kunming University of Science and Technology, Kunming, China, in 2018. His research interests include planetary penetrating, investigating and sampling, and planetary exploration robot systems.

RONGKAI LIU received the B.S. degrees in mechanical engineering from the Dalian Maritime University, Dalian, China, in 2017. He is currently pursuing the M.S. degree with the School of Mechatronics Engineering, Harbin Institute of Technology. His research interests include planetary penetrating, investigating, and sampling, and planetary exploration robot systems.

SHENGYUAN JIANG received the B.S. degree in mechanical metallurgy from the North China University of Technology, Beijing, China, in 1992, and the M.S. and Ph.D. degrees in mechanical design and theory from the School of Mechatronics Engineering, Harbin Institute of Technology, Harbin, China, in 1998 and 2001, respectively. Since 2011, he has been a Professor with the Department of Manufacturing Engineering for Aviation and Aerospace, Harbin Institute of Technology. His current research interests include planetary penetration, drilling and sampling techniques, aerospace system design, optimization, and simulation.